TECHNISCHE UNIVERSITÄT CHEMNITZ

Martin K. Bernauer Roland Herzog

Optimal Control of the Classical Two-Phase Stefan Problem in Level Set Formulation

CSC/10-04

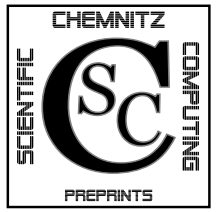

Chemnitz Scientific Computing Preprints

Chemnitz Scientific Computing Preprints – ISSN 1864-0087

Impressum:

Chemnitz Scientific Computing Preprints — ISSN 1864-0087

(1995–2005: Preprintreihe des Chemnitzer SFB393)

Herausgeber:
Professuren für
Numerische und Angewandte Mathematik
an der Fakultät für Mathematik
der Technischen Universität Chemnitz

Postanschrift:
TU Chemnitz, Fakultät für Mathematik
09107 Chemnitz
Sitz:
Reichenhainer Str. 41, 09126 Chemnitz

`http://www.tu-chemnitz.de/mathematik/csc/`

TECHNISCHE UNIVERSITÄT CHEMNITZ

Chemnitz Scientific Computing Preprints

Martin K. Bernauer Roland Herzog

Optimal Control of the Classical Two-Phase Stefan Problem in Level Set Formulation

CSC/10-04

Abstract

Optimal control (motion planning) of the free interface in classical two-phase Stefan problems is considered. The evolution of the free interface is modeled by a level set function. The first-order optimality system is derived on a formal basis. It provides gradient information based on the adjoint temperature and adjoint level set function. Suitable discretization schemes for the forward and adjoint systems are described. Numerical examples verify the correctness and flexibility of the proposed scheme.

CSC/10-04 ISSN 1864-0087 Oktober 2010

Contents

[23] S. Osher and J. A. Sethian. Fronts propagating with curvature-dependent speed. *Journal of Computational Physics*, 79:12–49, 1988. doi:10.1016/0021-9991(88)90002-2.

[24] I. Pawłow. Optimal control of two-phase Stefan problems—numerical solutions. In *Optimal Control of Partial Differential Equations, II (Oberwolfach, 1986)*, volume 78 of *Internationale Schriftenreihe Numerische Mathematik*, pages 179–206. Birkhäuser, Basel, 1987.

[25] B. Protas and W. Liao. Adjoint-based optimization of PDEs in moving domains. *Journal of Computational Physics*, 227:2707–2723, 2008. doi:10.1016/j.jcp.2007.11.014.

[26] J.-J. Xu and H.-K. Zhao. An Eulerian formulation for solving partial differential equations along a moving interface. *Journal of Scientific Computing*, 19(1-3):573–594, 2003. doi:10.1023/A:1025336916176.

[27] Z. Yang. *The Adjoint Method for the Inverse Design of Solidification Processes with Convection*. PhD thesis, Cornell University, 1997. Available from: http://mpdc.mae.cornell.edu/Publications/PDFiles/THESES/Yang.pdf.

[28] N. Zabaras, B. Ganapathysubramanian, and L. Tan. Modelling dendritic solidification with melt convection using the extended finite element method. *Journal of Computational Physics*, 218:200–227, 2006. doi:10.1016/j.jcp.2006.02.002.

[29] N. Zabaras, Y. Ruan, and O. Richmond. Design of two-dimensional Stefan processes with desired front motions. *Numerical Heat Transfer, Part B*, 21:307–325, 1992. doi:10.1080/10407799208944907.

1 Introduction

Many industrial applications lead to multiphysics models involving phase change phenomena. Important examples are the continuous casting of steel or crystal growth. Besides their practical importance, such phase change problems offer a broad spectrum of mathematical challenges, ranging from theoretical considerations concerning the well-posedness of such problems to the numerical simulation of phase change phenomena. In this work, we study a motion planning optimal control problem for the two-phase Stefan problem in level set formulation. We derive first-order necessary optimality conditions on a formal basis using tools from shape calculus, and discuss the discretization of the forward and adjoint problems. Numerical examples are also provided.

The two-phase Stefan problem is a classical model for phase change phenomena. It is based on the heat conduction equation in the solid and in the liquid phases. The motion of the interface (the freezing front) between these two phases is caused by a jump of the temperature gradient across the interface. The coupling of the interface motion to the heat equation is formulated as the Stefan condition.

We represent the moving boundary in terms of a level set function. One of the advantages of the level set formulation is its flexibility. It naturally handles closed interfaces and topological changes, in contrast to other models in which the interface is represented as the graph of a function or by a parametrization.

In the so called classical Stefan problem, an isotherm condition is used to prescribe the temperature on the moving interface. In this setup, the Stefan problem can be transformed into the enthalpy formulation, for which a solution theory based on weak solutions exists. The interface at any desired point in time can then be obtained in an a-posteriori step as the zero-level surface of the temperature. However, for the purpose of controlling the interface, we prefer the level set formulation in which the interface location appears as an extra state variable. This allows a natural formulation of motion planning problems, for example. Moreover, the level set function provides access to other geometric information such as the volume of the enclosed region and the curvature of the interface, for instance. The latter is essential when the isothermal condition at the interface is replaced by the Gibbs-Thomson correction, which relates the temperature at the interface to its curvature.

Before we review some existing approaches to the optimal control of the Stefan problem, let us explain our approach in more detail. As mentioned above, the model is based on the heat conduction equation in two phases. The motion of the interface between these two phases is captured by the level set method. The goal of the optimal control problem is to track a desired interface motion, which is provided in the form of a time-dependent signed distance function. This control goal is formulated in terms of a cost functional that measures the deviation of the actual from the desired interface and includes a control cost term. We use the associated Lagrange functional of the resulting optimal control problem to formally derive first-order optimality conditions. Shape calculus tools are used to handle the geometric variations. The resulting adjoint equation system has a similar structure as the forward two-phase Stefan problem. For the discretization of the forward and adjoint heat equations, we use the extended

finite element method of Chessa et al. [4]. The forward level set equation is discretized using a discontinuous Galerkin scheme [3]. The adjoint level set equation has a different structure than its counterpart in the forward system and it is treated with the discontinuous Galerkin scheme of Kuzmin [19]. Finally, a projected gradient algorithm is used to solve the optimal control problem subject to control constraints. We provide numerical examples which feature closed interfaces and topological changes in order to demonstrate the flexibility of this approach.

Let us now put our work into perspective. Hoffmann and Sprekels [15] consider a one-dimensional inverse two-phase Stefan problem. Their goal is to approximate an ideal interface motion by using a non-optimal feedback control law. The authors show the existence of a solution and provide numerical experiments. Niezgódka and Pawlow [21] discuss results on weak solutions of multidimensional Stefan problems in enthalpy formulation. In the companion paper [20], they use these results to show existence of optimal controls. Moreover, they discuss approximations of the optimal control problems under consideration. These approximation results are used to compute numerical solutions in [24]. Hoffmann et al. [14] treat the problem of a feedback control via thermostats for a multidimensional Stefan problem in enthalpy formulation. They do not present any numerical calculations. Knabner [18] uses a linearization technique for the control of one-dimensional Stefan problems. He carries out the minimization over a finite-dimensional subspace only, but is able to derive estimates of the order of convergence. After a discretization, the problem boils down to solving a least squares problem. The author presents several numerical examples. Zabaras and coworkers [29] discuss a design problem for two-dimensional Stefan problems. Their approach is based on a deforming finite element formulation. The authors assume that the desired interface location is known in the form of coordinates of nodes on the interface at distinct instances of time only. The boundary heat flux serves as the design variable. Kang and Zabaras [16] consider a similar design problem. Their goal is to find a boundary heat flux that realizes the desired interface motion by minimizing the defect between the reference temperature at the interface and the temperature at the actual interface. Their analysis consists of the derivation of a sensitivity problem and the corresponding adjoint problem. They use a deforming finite element method and a conjugate gradient algorithm for the numerical solution of the optimization problem. In their examples section, the authors present a unidirectional solidification problem and the problem of solidification in a corner. Yang [27] examines the inverse design of solidification problems with natural convection by minimizing a similar cost functional as Kang and Zabaras. However, his approach is tailored to unidirectional solidification and he assumes that the heat flux into the free boundary is known. He also uses a deforming finite element approach and an adjoint calculus for the solution of the optimization problem. Hinze and Ziegenbalg [12] represent the interface in a two-phase Stefan problem as the graph of a function over a rectangular domain, which allows for the direct control of the interface motion. They use the temperature at the boundary of the container as the control variable and aim to track the desired interface motion by minimizing an appropriate cost functional including an observation at terminal time. An adjoint equation system is derived in a formal way. This adjoint system is the basis for a gradient method with line search to solve the optimization problem.

[10] M. Fried. A level set based finite element algorithm for the simulation of dendritic growth. *Computing and Visualization in Science*, 2(2):97–110, 2004. doi:10.1007/s00791-004-0141-4.

[11] S. Gupta. *The Classical Stefan Problem. Basic Concepts, Modelling and Analysis*, volume 45 of *Applied Mathematics and Mechanics*. North-Holland, Amsterdam, 2003.

[12] M. Hinze and S. Ziegenbalg. Optimal control of the free boundary in a two-phase Stefan problem. *Journal of Computational Physics*, 223(2):657–684, 2007. doi:10.1016/j.jcp.2006.09.030.

[13] M. Hinze and S. Ziegenbalg. Optimal control of the free boundary in a two-phase Stefan problem with flow driven by convection. *ZAMM*, 87(6):430–448, 2007. doi:10.1002/zamm.200610326.

[14] K.-H. Hoffmann, M. Niezgódka, and J. Sprekels. Feedback control via thermostats of multidimensional two-phase Stefan problems. *Nonlinear Analysis*, 15(10):955–976, 1990. doi:10.1016/0362-546X(90)90078-U.

[15] K.-H. Hoffmann and J. Sprekels. Real-time control of the free boundary in a two-phase Stefan problem. *Numerical Functional Analysis and Optimization*, 5(1):47–76, 1982. doi:10.1080/01630568208816131.

[16] S. Kang and N. Zabaras. Control of the freezing interface motion in two-dimensional solidification processes using the adjoint method. *International Journal for Numerical Methods in Engineering*, 38:63–80, 1995. doi:10.1002/nme.1620380105.

[17] R. Kimmel and J. A. Sethian. Computing geodesic paths on manifolds. *Proceedings of the National Academy of Sciences of the United States of America*, 95(15):8431–8435, 1998.

[18] P. Knabner. Control of Stefan problems by means of linear-quadratic defect minimization. *Numerische Mathematik*, 46(3):429–442, 1985. doi:10.1007/BF01389495.

[19] D. Kuzmin. A vertex-based hierarchical slope limiter for p-adaptive discontinuous Galerkin methods. *Journal of Computational and Applied Mathematics*, 233(12):3077–3085, 2010. doi:10.1016/j.cam.2009.05.028.

[20] M. Niezgódka and I. Pawłow. Optimal control for parabolic systems with free boundaries. Existence of optimal controls, approximation results. In *Optimization Techniques (Proceedings of the Ninth IFIP Conference, Warsaw, 1979), Part 1*, volume 22 of *Lecture Notes in Computational Science and Engineering*, pages 412–420. Springer, Berlin, 1980. doi:10.1007/BFb0036420.

[21] M. Niezgódka and I. Pawłow. A generalized Stefan problem in several space variables. *Applied Mathematics and Optimization*, 9(3):193–224, 1982/83. doi:10.1007/BF01460125.

[22] J. Nocedal and S. Wright. *Numerical Optimization*. Springer, New York, 1999.

The extension to the time dependent case is again straightforward: The derivative of

$$J(\phi) := \int_0^T \int_{\{\phi(\cdot,t)=0\}} A\,\phi\,ds\,dt$$

in direction $\delta\phi$ is

$$D[\![J(\phi);\,\delta\phi]\!] = \int_0^T \int_{\Gamma(t)} A\,\delta\phi - \left(\frac{\partial}{\partial n}(A\,\phi) + \kappa\,A\,\phi\right)\frac{\delta\phi}{|\nabla\phi|}\,ds\,dt. \tag{B.7}$$

Again, if the integrand ψ is independent of λ (i.e., of ϕ), we have

$$D[\![J(\phi);\,\delta\phi]\!] = -\int_0^T \int_{\Gamma(t)} \left(\frac{\partial\psi}{\partial n} + \kappa\,\psi\right)\frac{\delta\phi}{|\nabla\phi|}\,ds\,dt. \tag{B.8}$$

References

[1] D. Adalsteinsson and J. A. Sethian. The fast construction of extension velocities in level set methods. *Journal of Computational Physics*, 148:2–22, 1999. doi:10.1006/jcph.1998.6090.

[2] M. K. Bernauer and R. Griesse. Implementation of an X-FEM solver for the classical two-phase Stefan problem. *submitted*, 2009.

[3] Y. Cheng and C.-W. Shu. A discontinuous Galerkin finite element method for directly solving the Hamilton-Jacobi equations. *Journal of Computational Physics*, 223(1):398–415, 2007. doi:10.1016/j.jcp.2006.09.012.

[4] J. Chessa, P. Smolinski, and T. Belytschko. The extended finite element method (XFEM) for solidification problems. *International Journal for Numerical Methods in Engineering*, 53(8):1959–1977, 2002. doi:10.1002/nme.386.

[5] M. Delfour and J.-P. Zolésio. *Shapes and Geometries. Analysis, Differential Calculus, and Optimization*. SIAM, Philadelphia, 2001.

[6] G. Dziuk and C. M. Elliott. Finite elements on evolving surfaces. *IMA Journal of Numerical Analysis*, 27(2):262–292, 2007. doi:10.1093/imanum/drl023.

[7] G. Dziuk and C. M. Elliott. An Eulerian approach to transport and diffusion on evolving implicit surfaces. *Computing and Visualization in Science*, 13(1):17–28, 2008. doi:10.1007/s00791-008-0122-0.

[8] C. Eck, H. Garcke, and P. Knabner. *Mathematische Modellierung*. Springer Lehrbuch. Springer-Verlag, Berlin Heidelberg, 2008.

[9] R. Fosdick and H. Tang. Surface transport in continuum mechanics. *Mathematics and Mechanics of Solids*, 14(6):587–598, 2009. doi:10.1177/1081286507087316.

The discretization of the infinite dimensional problems is carried out by a finite difference approach. The authors present a numerical example to verify their theoretical results. Later, the same authors extend this approach and include convection-driven flows in the liquid phase [13]. Protas and Liao [25] consider a one-dimensional optimization problem for a PDE system in a moving domain. The authors map the moving domain into a fixed domain and then derive an adjoint equation system. Alternatively, they show how to derive an adjoint system directly in the moving domain using methods of non-cylindrical calculus. These two approaches do not commute. The numerical examples given in this paper are based on a spectral discretization. The authors also discuss the consistency of their gradient approximation.

Our approach is similar to [12] in several aspects:

- We also treat the classical Stefan problem with a sharp representation of the interface. Convection in the fluid phase is neglected.
- A formal Lagrange approach is used to derive an adjoint equation system.
- The optimization problem is solved by a gradient algorithm.

The main differences of our work to [12] are:

- We use a level set formulation to represent the moving interface, and thus closed interfaces and topological changes can be handled naturally.
- The derivation of the adjoint equation system makes use of shape calculus tools.
- Our numerical approach is based on the extended finite element method (which operates on a fixed mesh) and discontinuous Galerkin schemes.

The material in this paper is organized as follows. In Section 2, we discuss the model equations and the geometric setup. An optimal control problem that aims to track a desired interface motion is formulated in Section 3. We also include a brief discussion of the adjoint equation system there. The derivation of this system is contained in Appendix A. We start Section 4 with a brief review of the discretization of the Stefan problem, but refer to [2] for the details. The remainder of this section is devoted to the discretization of the adjoint equation system. We include a detailed algorithm that describes the solver. Finally, we present two numerical examples in Section 5. The first example includes control constraints while in the second example we demonstrate the ability of our approach to handle topological changes. In Appendix B, we collect several results from shape calculus that we need in Appendix A to derive the adjoint system.

2 Model Equations

The solidification of a material in a fixed domain $D \subset \mathbb{R}^2$ (the hold-all) is modeled by the two-phase Stefan problem. It can be formulated in the following way [11, p. 23ff]:

Find a function $y : D \times [0,T] \to \mathbb{R}$ (the temperature) and a function $\phi : D \times [0,T] \to \mathbb{R}$ such that (see Figure 2.1)

$$\begin{aligned}
\rho\, c_S\, y_t - k_S\, \Delta y &= f && \text{in } \Omega_S(t) && (2.1a)\\
\rho\, c_F\, y_t - k_F\, \Delta y &= f && \text{in } \Omega_F(t) && (2.1b)\\
y(x,0) &= y_0(x) && \text{in } D && (2.1c)\\
k_S \tfrac{\partial y}{\partial n} &= u && \text{on } \Gamma_C && (2.1d)\\
k_S \tfrac{\partial y}{\partial n} &= g && \text{on } \Gamma_N && (2.1e)\\
y(x,t) &= y_M && \text{on } \Gamma_I(t) && (2.1f)\\
-\rho\, L\, \phi_t &= \left[k\, \nabla y\right]_F^S \cdot \nabla \phi && \text{on } \Gamma_I(t) && (2.1g)\\
\phi(x,0) &= \phi_0(x) && \text{in } D && (2.1h)
\end{aligned}$$

on a certain time horizon $[0,T]$.

The interface $\Gamma_I(t)$ is defined as the zero level set of ϕ:

$$\Gamma_I(t) = \{x \mid \phi(x,t) = 0\} = \{\phi(\cdot,t) = 0\}\,.$$

It divides D into $\Omega_S(t) = \{\phi(\cdot,t) < 0\}$, occupied by the solid phase, and $\Omega_F(t) = \{\phi(\cdot,t) > 0\}$, occupied by the fluid phase. This choice of sign implies that

$$n = \tfrac{\nabla \phi}{|\nabla \phi|} \tag{2.2}$$

is the outward unit normal to $\Omega_S(t)$. The boundary of the hold-all D is decomposed into two parts

$$\partial D = \Gamma_C \cup \Gamma_N, \quad \Gamma_C \cap \Gamma_N = \emptyset.$$

The part Γ_C, which we require to be non-empty, refers to the part of the boundary on which the control u is applied, while a prescribed heat flux g acts on Γ_N which might be empty.

We require that the density of the material, ρ, is constant and equal in both phases so that we can ignore mass transport effects. $c_P \in \mathbb{R}\,(P \in \{S,F\})$ is the specific heat at constant pressure, $k_P \in \mathbb{R}\,(P \in \{S,F\})$ is the coefficient of heat conduction and $y_M \in \mathbb{R}$ is the reference temperature at which solidification takes place. L denotes the latent heat that is released upon solidification.

The Stefan condition (2.1g) can be equivalently expressed as [11, Section 1.4]

$$\rho\, L\, V \cdot n = \left[k\, \nabla y\right]_F^S \cdot n \qquad \text{on } \Gamma_I(t). \tag{2.3}$$

It states that the normal velocity $V \cdot n$ of $\Gamma_I(t)$ is proportional to the jump of the normal derivative of the temperature:

$$\left[k\, \nabla y\right]_F^S = k_S \nabla y\big|_{\Omega_S(t)} - k_F \nabla y\big|_{\Omega_F(t)}.$$

and the derivative of the functional

$$J(\phi) = \int_{\{\phi<0\}} f\, dx$$

in direction $\delta\phi$ is given by

$$D\,[\![J(\phi);\, \delta\phi]\!] = -\int_\Gamma f \frac{\delta\phi}{|\nabla\phi|}\, ds.$$

The extension to the time-dependent case $\phi = \phi(x,t)$ is straightforward. In this case, the derivative of the functional

$$J(\phi) = \int_0^T \int_{\{\phi(\cdot,t)<0\}} f\, dx\, dt$$

in direction $\delta\phi$ is given by

$$D\,[\![J(\phi);\, \delta\phi]\!] = -\int_0^T \int_{\Gamma(t)} f \frac{\delta\phi}{|\nabla\phi|}\, ds\, dt. \tag{B.6}$$

B.4 Derivatives of Boundary Integrals

We denote by Γ_λ the boundary of the perturbed set Ω_λ that depends on the parameter λ. Note that $\Omega_0 = \Omega$ and $\Gamma_0 = \Gamma = \partial\Omega$. We define the functional

$$J(\lambda) := \int_{\Gamma_\lambda} \psi(\lambda, x)\, ds.$$

The derivative of J at $\lambda = 0$ is given by [5, Theorem 4.3, p. 355]

$$dJ(0) = \int_\Gamma \psi'(0) + \left(\frac{\partial \psi}{\partial n} + \kappa\, \psi\right) V(0) \cdot \vec{n}\, ds,$$

where $\psi'(0)(x) = \frac{\partial \psi}{\partial \lambda}(0,x)$.

This translates to the level set context by the settings

$$\Gamma_\lambda = \{\phi + \lambda\, \delta\phi = 0\}\,, \quad \psi(\lambda) = A(\phi + \lambda\, \delta\phi)$$

for some linear operator A as follows. The derivative of the functional

$$J(\phi) := \int_{\{\phi=0\}} A\, \phi\, ds$$

in direction $\delta\phi$ is given by

$$D\,[\![J(\phi);\, \delta\phi]\!] = \int_\Gamma A\, \delta\phi - \left(\frac{\partial}{\partial n}(A\, \phi) + \kappa\, A\, \phi\right) \frac{\delta\phi}{|\nabla\phi|}\, ds.$$

If the integrand ψ is independent of λ (i.e., of ϕ), we have

$$D\,[\![J(\phi);\, \delta\phi]\!] = -\int_\Gamma \left(\frac{\partial \psi}{\partial n} + \kappa\, \psi\right) \frac{\delta\phi}{|\nabla\phi|}\, ds.$$

$$- \int_0^T \int_{\Omega(t)} g(x,t) \frac{\partial h}{\partial t}(x,t)\, dx\, dt \tag{B.3}$$
$$- \int_0^T \int_{\Gamma(t)} g(x,t)\, h(x,t)\, \mathbf{w}(x,t) \cdot n(x,t)\, ds\, dt.$$

For more details concerning Reynold's Transport Theorem and a proof we refer to [8, Section 5.4].

B.2 A Moving Surface Transport Theorem

Let $f(\cdot) : \Gamma(t) \to \mathbb{R}$ be a scalar quantity that is defined on the moving surface $\Gamma(t)$ and let $\mathbf{w}(x,t)$ be the velocity field with which $\Gamma(t)$ moves. Then

$$\frac{d}{dt} \int_{\Gamma(t)} f(x,t)\, ds = \int_{\Gamma(t)} \mathring{f}(x,t) + f(x,t)\, \operatorname{div}_{\Gamma(t)}\big(\mathbf{w}(x,t)\big)\, ds. \tag{B.4}$$

If f is the restriction of a globally defined quantity $\hat{f}$ to $\Gamma(t)$, the material derivative can be equivalently expressed as

$$\mathring{f}(x,t) = \frac{\partial \hat{f}}{\partial t}(x,t) + \nabla \hat{f}(x,t) \cdot \mathbf{w}(x,t).$$

Just like above, we set $f(x,t) = g(x,t)\, h(x,t)$ and obtain a formula for integration-by-parts on time-varying surfaces:

$$\begin{aligned} \int_0^T \int_{\Gamma(t)} \hat{g}(x,t)\, \hat{h}_t(x,t)\, ds\, dt = \int_{\Gamma(T)} g(x,T)\, h(x,T)\, ds - \int_{\Gamma(0)} g(x,0)\, h(x,0)\, ds \\ - \int_0^T \int_{\Gamma(t)} \hat{g}_t(x,t)\, \hat{h}(x,t) + \mathbf{w}(x,t) \cdot \nabla\big(\hat{g}(x,t)\, \hat{h}(x,t)\big) \\ + g(x,t)\, h(x,t)\, \operatorname{div}_{\Gamma(t)} \mathbf{w}(x,t)\, ds\, dt. \end{aligned} \tag{B.5}$$

More details on this surface transport theorem can be found in [9].

B.3 Derivatives of Domain Integrals

Let $\Omega \subset D$ for a fixed hold-all D, denote $\Gamma = \partial\Omega$ and let $J(\Omega) = \int_\Omega f(x)\, dx$. The perturbation of this functional with respect to a certain velocity field V is given by [5, Theorem 4.2, p. 352]

$$dJ(\Omega; V) = \int_\Gamma f(x)\, \langle V(0), n \rangle\, ds.$$

If Γ is given by the zero level set of a function ϕ and $\Omega = \{x \,|\, \phi(x) < 0\}$, the velocity has to be chosen as

$$V(0) = -\frac{\delta\phi}{|\nabla\phi|} \frac{\nabla\phi}{|\nabla\phi|},$$

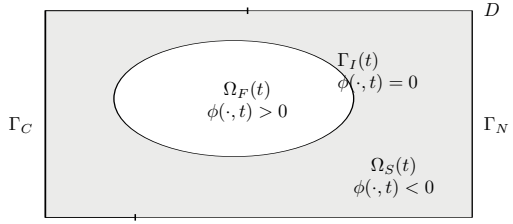

Figure 2.1: Setup of geometry for the two-phase Stefan problem.

3 The Optimal Control Problem and Optimality Conditions

The objective functional

$$J(y,\phi,u) = \frac{\gamma_1}{2} \int_0^T \int_{\Gamma_I(t)} |\phi_d|^2\, ds\, dt + \frac{\gamma_2}{2} \int_{\Gamma_I(T)} |\phi_T|^2\, ds + \frac{\gamma_3}{2} \int_0^T \int_{\Gamma_C} |u|^2\, ds\, dt$$

is of tracking type. It aims to control the motion of the interface over the control horizon $[0,T]$ and to monitor the final position at terminal time T. The last term represents control costs that are added for regularization purposes.

Remark 3.1 *1. If ϕ_d is chosen as the signed distance function to a desired interface position then the terms*

$$\int_{\Gamma_I(t)} |\phi_d|^2\, ds \quad \text{and} \quad \int_{\Gamma_I(T)} |\phi_T|^2\, ds$$

express the accumulated squared distance of the current interface from the desired interface at time $t \in [0,T]$. Note that this is independent of the choice of ϕ away from $\Gamma_I(t)$.

2. This objective functional can be extended by terms such as

$$\int_0^T \int_D |y - y_d|^2\, dx\, dt \quad \text{and} \quad \int_D |y(T) - y_T|^2\, dx$$

for the tracking of a desired temperature profile y_d and y_T but we omit them for the sake of brevity.

Finally, we formulate our motion planning problem as

$$\min_{y,\phi,u} J(y,\phi,u) \quad \text{subject to} \quad (2.1). \tag{MPP}$$

We comment on the inclusion of control constraints below.

Remark 3.2 *Note that the level set function ϕ carrying the geometric information is a state variable. Thus, (MPP) is an optimal control problem for a free boundary problem, rather than a shape optimization problem.*

We assume that each choice of the control u induces unique states $y(u)$ and $\phi(u)$. Thus we introduce the reduced cost functional $\widehat{J}(u) := J(y(u), \phi(u), u)$ and consider the unconstrained problem

$$\min_u \widehat{J}(u).$$

To compute the gradient of $\widehat{J}(u)$, we introduce the Lagrange functional to (MPP) (We omit the ds, dx and dt for the sake of brevity.)

$$\begin{aligned}\mathcal{L}(y,\,\phi,\,u,\,p,\,p_C,\,p_N,\,p_I,\,\psi) &= J(y,\phi,u) - \int_0^T \int_D (-f)\,p \\ &- \int_0^T \int_{\Omega_S(t)} \left(\rho\, c_S\, y_t - k_S\, \triangle y\right) p - \int_0^T \int_{\Omega_F(t)} \left(\rho\, c_F\, y_t - k_F\, \triangle y\right) p \\ &- \int_0^T \int_{\Gamma_N} \left(k_S \tfrac{\partial y}{\partial n_S} - g\right) p_N - \int_0^T \int_{\Gamma_C} \left(k_S \tfrac{\partial y}{\partial n_S} - u\right) p_C \\ &- \int_0^T \int_{\Gamma_I(t)} (y - y_M)\, p_I - \int_0^T \int_{\Gamma_I(t)} \left(\rho\, L\, \phi_t + \left[k\, \nabla y\right]_F^S \cdot \nabla \phi\right)\, \psi.\end{aligned}$$

The following adjoint equation system results from setting $\mathcal{L}_y(\cdot) = \mathcal{L}_\phi(\cdot) = 0$. For a detailed derivation we refer to Appendix A.

$$\begin{aligned}
-\rho\, c_S\, p_t - k_S\, \triangle p &= 0 && \text{in } \Omega_S(t) && \text{(3.1a)}\\
-\rho\, c_F\, p_t - k_F\, \triangle p &= 0 && \text{in } \Omega_F(t) && \text{(3.1b)}\\
\rho\, c_S\, p(T) &= 0 && \text{in } \Omega_S(T) && \text{(3.1c)}\\
\rho\, c_F\, p(T) &= 0 && \text{in } \Omega_F(T) && \text{(3.1d)}\\
p_C = p, \quad k_S \tfrac{\partial p}{\partial n} &= 0 && \text{on } \Gamma_C && \text{(3.1e)}\\
p_N = p, \quad k_S \tfrac{\partial p}{\partial n} &= 0 && \text{on } \Gamma_N && \text{(3.1f)}\\
\rho \left[c\right]_F^S p\, V \cdot n - \left[k\, \nabla p\right]_F^S \cdot n_S &= p_I && \text{on } \Gamma_I(t) && \text{(3.1g)}\\
p &= \psi\, |\nabla \phi| && \text{on } \Gamma_I(t) && \text{(3.1h)}\\
-\hat{L}\left(\psi_t + \operatorname{div}(\psi\, V)\right) - \tfrac{\partial y}{\partial n}\, p_I &= -\tfrac{\gamma_1}{2}\left(\tfrac{\partial}{\partial n}|\phi_d|^2 + \kappa\, |\phi_d|^2\right) && \text{on } \Gamma_I(t) && \text{(3.1i)}\\
\hat{L}\, \psi(T) &= -\tfrac{\gamma_2}{2}\left(\tfrac{\partial}{\partial n}|\phi_T|^2 + \kappa\, |\phi_T|^2\right) && \text{on } \Gamma_I(T) && \text{(3.1j)}\\
\hat{L} &:= \rho\, L\, |\nabla \phi|. && && \text{(3.1k)}
\end{aligned}$$

We refer to p and ψ as the adjoint temperature and adjoint level set function, respectively. Equations (3.1a)–(3.1f) have a similar structure as the corresponding equations (2.1a)–(2.1e) in the forward system. As expected, the time direction is reversed in the adjoint equations. The boundary conditions for p are homogeneous and of Neumann type on ∂D. Equation (3.1g) is of Stefan type and states that the multiplier p_I can be expressed in terms of p. V is the velocity field with which the interface moves as defined in (2.3). The coupling between the two adjoint states p and ψ is enforced by the interface condition (3.1h) that completes the adjoint heat equation. Note that this equation plays the same role as (2.1f) in the forward system. Finally, equations (3.1i)–(3.1j) constitute the adjoint Stefan condition. The forcing terms on the right hand sides of both equations are contributions from the cost functional J.

Requiring $\mathcal{L}_\phi\, \delta\phi = 0$ for all admissible directions $\delta\phi$ results in the equations:

$$\begin{aligned}
-\rho\, L\, |\nabla\phi|\, \psi_t &= -\frac{\gamma_2}{2}\left(\frac{\partial}{\partial n}\left(|\phi_d|^2\right) + \kappa\, |\phi_d|^2\right) + \frac{\partial y}{\partial n}\, p_I + |\nabla\phi|\, \rho\, L\, \nabla\psi \cdot V && \text{(A.3a)}\\
&\quad + \psi\, \left[\frac{\partial}{\partial n}(\rho\, L\, \phi_t + \left[k\, \nabla y\right]_F^S \cdot \nabla\phi) + |\nabla\phi|\, \rho\, L\, \operatorname{div}_{\Gamma_I(t)} V\right], \\
\psi(T) &= -\frac{1}{\rho\, L\, |\nabla\phi|}\, \frac{\gamma_4}{2}\left(\frac{\partial}{\partial n}\left(|\phi_T|^2\right) + \kappa\, |\phi_T|^2\right). && \text{(A.3b)}
\end{aligned}$$

During all our computations, V is always constructed by a constant extension of (2.3) in normal direction. As a consequence, we have

$$\operatorname{div}_{\Gamma_I(t)} V = \operatorname{div} V,$$

and this allows us to write

$$\nabla\psi \cdot V + \psi\, \operatorname{div}_{\Gamma_I(t)} V = \nabla\psi \cdot V + \psi\, \operatorname{div} V = \operatorname{div}\left(\psi\, V\right).$$

In addition, the level set equation we use to evolve ϕ corresponds to the Stefan condition (2.1g) with a proper extension of the jump of the temperature gradients. This means that

$$\frac{\partial}{\partial n}(\rho\, L\, \phi_t + \left[k\, \nabla y\right]_F^S \cdot \nabla\phi) = 0$$

holds on all of D or at least in the narrow band that we use for the level set computations. Thus, we can omit this term from the derivative and the final version of the adjoint Stefan condition (3.1i) with terminal condition (3.1j) follows.

B Transport Theorems and Shape Calculus

In this section, we collect transport theorems and shape calculus tools that are needed to derive the adjoint equation system (3.1). We state these results without the precise regularity assumptions.

B.1 Reynold's Transport Theorem

Let $\mathbf{w}(x,t)$ be the velocity field with which the control volume $\Omega(t)$ moves and let $\Gamma(t) = \partial\Omega(t)$. Then

$$\begin{aligned}
\frac{d}{dt}\int_{\Omega(t)} f(x,t)\, dx &= \int_{\Omega(t)} \frac{\partial f}{\partial t}(x,t) + \operatorname{div}\left(f(x,t)\, \mathbf{w}(x,t)\right) dx && \text{(B.1)}\\
&= \int_{\Omega(t)} \frac{\partial f}{\partial t}(x,t)\, dx + \int_{\Gamma(t)} f(x,t)\, \mathbf{w}(x,t) \cdot n(x,t)\, ds. && \text{(B.2)}
\end{aligned}$$

If we set $f(x,t) = g(x,t)\, h(x,t)$ and integrate over the time interval $[0,T]$, a formula for integration-by-parts in time-varying domains follows:

$$\int_0^T \int_{\Omega(t)} \frac{\partial g}{\partial t}(x,t)\, h(x,t)\, dx\, dt = \int_{\Omega(T)} g(x,T)\, h(x,T)\, dx - \int_{\Omega(0)} g(x,0)\, h(x,0)\, dx$$

To further simplify the second part of this formula, we invoke the surface transport theorem (B.5):

$$\begin{aligned}
\int_0^T \int_{\Gamma_I(t)} \rho\, L\, \delta\phi_t\, \psi &= \int_{\Gamma_I(T)} \rho\, L\, \delta\phi\, \psi - \int_{\Gamma_I(0)} \rho\, L\, \delta\phi\, \psi \\
&\quad - \int_0^T \int_{\Gamma_I(t)} \rho\, L\, \delta\phi\, \psi_t + \nabla(\rho\, L\, \delta\phi\, \psi) \cdot V + \rho\, L\, \delta\phi\, \psi\, \operatorname{div}_{\Gamma_I(t)}(V) \\
&= \int_{\Gamma_I(T)} \rho\, L\, \delta\phi\, \psi - \int_{\Gamma_I(0)} \rho\, L\, \delta\phi\, \psi - \int_0^T \int_{\Gamma_I(t)} \rho\, L\, \delta\phi\, \psi_t \\
&\quad - \int_0^T \int_{\Gamma_I(t)} \delta\phi\, \rho\, L\, \left(\nabla\psi \cdot V + \psi\, \operatorname{div}_{\Gamma_I(t)} V\right) \\
&\quad - \int_0^T \int_{\Gamma_I(t)} \rho\, L\, \psi\, \nabla\delta\phi \cdot V.
\end{aligned}$$

The last term cancels with some of the other contributions in (A.2):

$$\begin{aligned}
&-\rho\, L\, \psi\, \nabla\delta\phi \cdot V + (k_S \nabla y \cdot \nabla\delta\phi - k_F\, \nabla y \cdot \nabla\delta\phi)\, \psi \\
&\qquad = \psi\, \left(-(k_S \nabla y - k_F\, \nabla y)\, \nabla\delta\phi + (k_S \nabla y - k_F\, \nabla y)\, \nabla\delta\phi\right) = 0. \qquad \diamond
\end{aligned}$$

Using $\delta\phi(x,0) = 0$, we end up with the following derivative of $\mathcal{L}$ in direction $\delta\phi$:

$$\begin{aligned}
\mathcal{L}_\phi\, \delta\phi &= -\frac{\gamma_1}{2} \int_0^T \int_{\Gamma_I(t)} \frac{\delta\phi}{|\nabla\phi|} \left(\frac{\partial}{\partial n}\left(|\phi_d|^2\right) + \kappa\, |\phi_d|^2\right) \\
&\quad - \frac{\gamma_2}{2} \int_{\Gamma_I(T)} \frac{\delta\phi(T)}{|\nabla\phi|} \left(\frac{\partial}{\partial n}\left(|\phi_T|^2\right) + \kappa\, |\phi_T|^2\right) \\
&\quad + \int_0^T \int_{\Gamma_I(t)} \frac{\delta\phi}{|\nabla\phi|} f\, p - \int_0^T \int_{\Gamma_I(t)} \frac{\delta\phi}{|\nabla\phi|} f\, p + \int_0^T \int_{\Gamma_I(t)} \frac{\delta\phi}{|\nabla\phi|} \frac{\partial y}{\partial n}\, p_I \\
&\quad + \int_0^T \int_{\Gamma_I(t)} \frac{\delta\phi}{|\nabla\phi|} \frac{\partial}{\partial n}(\rho\, L\, \phi_t + \left[k\, \nabla y\right]_F^S \cdot \nabla\phi)\, \psi \\
&\quad - \left\{ \int_{\Gamma_I(T)} \rho\, L\, \delta\phi\, \psi - \int_{\Gamma_I(0)} \rho\, L\, \delta\phi\, \psi - \int_0^T \int_{\Gamma_I(t)} \rho\, L\, \delta\phi\, \psi_t \right. \\
&\quad \left. - \int_0^T \int_{\Gamma_I(t)} \delta\phi\, \rho\, L\, \left(\nabla\psi \cdot V + \psi\, \operatorname{div}_{\Gamma_I(t)} V\right) \right\} \\
&= -\frac{\gamma_1}{2} \int_0^T \int_{\Gamma_I(t)} \frac{\delta\phi}{|\nabla\phi|} \left(\frac{\partial}{\partial n}\left(|\phi_d|^2\right) + \kappa\, |\phi_d|^2\right) + \int_0^T \int_{\Gamma_I(t)} \frac{\delta\phi}{|\nabla\phi|} \frac{\partial y}{\partial n}\, p_I \\
&\quad + \int_0^T \int_{\Gamma_I(t)} \frac{\delta\phi}{|\nabla\phi|} \frac{\partial}{\partial n}(\rho\, L\, \phi_t + \left[k\, \nabla y\right]_F^S \cdot \nabla\phi)\, \psi \\
&\quad + \int_0^T \int_{\Gamma_I(t)} \rho\, L\, \delta\phi\, \psi_t + \int_0^T \int_{\Gamma_I(t)} \delta\phi\, \rho\, L\, \left(\nabla\psi \cdot V + \psi\, \operatorname{div}_{\Gamma_I(t)} V\right) \\
&\quad - \frac{\gamma_2}{2} \int_{\Gamma_I(T)} \frac{\delta\phi(T)}{|\nabla\phi|} \left(\frac{\partial}{\partial n}\left(|\phi_T|^2\right) + \kappa\, |\phi_T|^2\right) - \int_{\Gamma_I(T)} \rho\, L\, \delta\phi\, \psi.
\end{aligned}$$

Remark 3.3 *1. If tracking terms for a desired temperature profile y_d are included in the cost functional as suggested in Remark 3.1–(2), additional forcing terms appear on the right hand sides of (3.1a)–(3.1d).*

2. Note that we do not require ϕ to be a signed distance function to the interface $\Gamma_I(t)$. If it is, then $|\nabla\phi| = 1$ holds in (3.1).

The gradient equation

$$0 = \gamma_3\, u + p \qquad \text{on } \Gamma_C \tag{3.2}$$

is obtained by taking the derivative $\mathcal{L}_u\, \delta u$.

Remark 3.4 *Frequently, the control u is restricted to belong to a convex set $\mathcal{U}_{ad}$ of admissible controls. In this case, the gradient equation (3.2) has the form*

$$\mathcal{L}_u(v-u) = \int_0^T \int_{\Gamma_C} (\gamma_3\, u + p)\, (v-u)\, ds\, dt \geq 0 \quad \forall v \in \mathcal{U}_{ad}.$$

The adjoint equation system (3.1) remains unchanged.

An algorithm for the solution of (MPP) based on this gradient equation and the adjoint system (3.1) is stated in Algorithm 1. Note that pointwise control constraints $\mathcal{U}_{\text{ad}} = \{u_a \leq u \leq u_b\}$ are present.

Algorithm 1 Adjoint-Based Projected Gradient Method

Input: u^0
Output: $\widehat{u}, \widehat{y}, \widehat{\phi}, \widehat{p}, \widehat{\psi}$

1: $j = 0$
2: **while** the convergence condition is not fulfilled **do**
3: Solve the forward problem (2.1) for y^j and ϕ^j.
4: Solve the adjoint problem (3.1) for p^j and ψ^j.
5: Construct the descent direction from (3.2)

$$v^j = -(\gamma_3\, u^j + p^j).$$

6: Determine σ^j from

$$\sigma^j := \arg\min_{\sigma} \widehat{J}\big(\mathcal{P}_{[u_a,u_b]}(u^j + \sigma\, v^j)\big).$$

7: Set $u^{j+1} = \mathcal{P}_{[u_a,u_b]}(u^j + \sigma^j\, v^j)$, $j \to j+1$.
8: **end while**

Remark 3.5 *1. Steps 3 and 4 require the discretization of the coupled equation systems (2.1) and (3.1). This is discussed in Section 4.*

2. The choice of v^j in Step 5 corresponds to the negative gradient, i.e., the direction of steepest descent.

3. *The projection $\mathcal{P}_{[u_a,u_b]}$ in steps 6 and 7 ensures that the computed controls are admissible. It is defined as*

$$\mathcal{P}_{[u_a,u_b]}(u) = \min\{u_b, \max\{u_a, u\}\}.$$

4. *Step 6 can not be implemented exactly. Instead, a line search procedure, e.g. the Armijo rule with backtracking is used to determine an approximation to σ^j, see, e.g., [22, Chapter 3].*

4 Discretization of the Forward and Adjoint Systems

4.1 Discretization of the Forward Problem

The discretization of the coupled PDE system (2.1) bears several difficulties.

4.1.1 Tracking/Capturing the Moving Interface

We use the level set method [23] to represent the moving interface $\Gamma_I(t)$, which handles closed curves and topological changes naturally. The idea of this approach is to extend (2.1g) to all of D or at least to a neighborhood of $\Gamma_I(t)$ by the techniques explained in Section 4.1.2 below. This results in the first oder PDE (the so called level set equation)

$$\phi_t + V \cdot \nabla\phi = 0 \qquad \text{in } D \tag{4.1a}$$
$$\phi(x,0) = \phi_0 \qquad \text{in } D \tag{4.1b}$$

that we discretize in space by adopting the discontinuous Galerkin scheme from [3]. The time discretization is realized by an explicit Runge-Kutta method.

4.1.2 Reinitialization of the Level Set Function/Extension of Interfacial Quantities

As indicated above, the level set technique requires the extension of quantities given on an interface to a neighborhood of that interface. The standard approach is to compute a constant extension in normal direction. Owing to the relation (2.2), this amounts to solving the PDE [1]

$$\operatorname{sign}(\phi)\, \nabla\Psi \cdot \nabla\phi = 0 \qquad \text{in } D \tag{4.2a}$$
$$\Psi = \bar{\Psi} \qquad \text{on } \Gamma_I(t) \tag{4.2b}$$

for Ψ, where $\bar{\Psi}$ are the given data on the interface. On a triangular grid, (4.2) can be solved efficiently by the fast marching method of Kimmel and Sethian [17]. Theoretically, this extension fails, e.g., in the presence of corners in the interface as the normal to $\Gamma_I(t)$ is not well-defined in a whole region in this situation. However, this effect can be ignored in practical computations, and the resulting extended quantity is always continuous. The signed distance function to the current interface comes as a side-product of this extension process. This allows for a cheap reinitialization of the level set function in order to maintain its signed distance property.

$$= \int_0^T \int_{\Gamma_I(t)} \frac{\delta\phi}{|\nabla\phi|} \big(\rho\, c_F\, y_t - k_F\, \triangle y\big)\, p = \int_0^T \int_{\Gamma_I(t)} \frac{\delta\phi}{|\nabla\phi|} f\, p,$$

where the last equality holds again in the sense of a trace because of (2.1b). ◇

(A.1e) and (A.1f)

The boundary integrals in these terms are independent of ϕ and thus their derivatives vanish. ◇

(A.1g)

To compute the contribution of this term we assume that p_I is defined on all of D, i.e., we interpret p_I as the restriction of a globally defined quantity to $\Gamma_I(t)$. This allows us to apply the shape calculus tools from Appendix B.

Using (B.8), we conclude

$$\begin{aligned}
(\text{A.1g}) &= -\int_0^T \int_{\Gamma_I(t)} \frac{\delta\phi}{|\nabla\phi|} \left(\frac{\partial\big((y - y_M)\, p_I\big)}{\partial n} + \kappa\, (y - y_M)\, p_I \right) \\
&= -\int_0^T \int_{\Gamma_I(t)} \frac{\delta\phi}{|\nabla\phi|} \left(\frac{\partial (y - y_M)}{\partial n}\, p_I \right) && \text{by (2.1f)} \\
&= -\int_0^T \int_{\Gamma_I(t)} \frac{\delta\phi}{|\nabla\phi|} \frac{\partial y}{\partial n}\, p_I. && \diamond
\end{aligned}$$

(A.1h)

To compute the variation of the Stefan condition we assume that ψ and the jump of the temperature gradients $\big[k\,\nabla y\big]_F^S$ are defined on all of D for the same reason as in the last paragraph.

As the integrand is of the form $\psi\, A(\phi + \delta\phi)$ with a linear operator A, we are in the position to apply (B.7) and infer

$$\begin{aligned}
(\text{A.1h}) &= -\int_0^T \int_{\Gamma_I(t)} \frac{\delta\phi}{|\nabla\phi|} \left(\frac{\partial}{\partial n} \big((\rho\, L\, \phi_t + \big[k\,\nabla y\big]_F^S \cdot \nabla\phi)\, \psi \big) \right. \\
&\qquad \left. + \kappa\, (\rho\, L\, \phi_t + \big[k\,\nabla y\big]_F^S \cdot \nabla\phi)\, \psi \right) \\
&\quad + \int_0^T \int_{\Gamma_I(t)} (\rho\, L\, \delta\phi_t + k_S \nabla y \cdot \nabla\delta\phi - k_F\, \nabla y \cdot \nabla\delta\phi)\, \psi \\
&= -\int_0^T \int_{\Gamma_I(t)} \frac{\delta\phi}{|\nabla\phi|} \frac{\partial}{\partial n} \big(\rho\, L\, \phi_t + \big[k\,\nabla y\big]_F^S \cdot \nabla\phi\big)\, \psi && \text{by (2.1g)} \\
&\quad + \int_0^T \int_{\Gamma_I(t)} (\rho\, L\, \delta\phi_t + k_S \nabla y \cdot \nabla\delta\phi - k_F\, \nabla y \cdot \nabla\delta\phi)\, \psi. && (\text{A.2})
\end{aligned}$$

$$D\left[\!\!\left[\int_0^T \int_{\Gamma_N} \left(k_S \tfrac{\partial y}{\partial n} - g\right) p;\, \delta\phi \right]\!\!\right] - \tag{A.1e}$$

$$D\left[\!\!\left[\int_0^T \int_{\Gamma_C} \left(k_S \tfrac{\partial y}{\partial n} - u\right) p;\, \delta\phi \right]\!\!\right] - \tag{A.1f}$$

$$D\left[\!\!\left[\int_0^T \int_{\Gamma_I(t)} (y - y_M)\, p_I;\, \delta\phi \right]\!\!\right] - \tag{A.1g}$$

$$D\left[\!\!\left[\int_0^T \int_{\Gamma_I(t)} \left(\rho\, L\, \phi_t + \left[k\, \nabla y\right]_F^S \cdot \nabla\phi\right) \psi;\, \delta\phi \right]\!\!\right]. \tag{A.1h}$$

(A.1a)

The contributions of the cost functional are (see (B.8))

$$\begin{aligned} &D\left[\!\!\left[\frac{\gamma_1}{2}\int_0^T \int_{\Gamma_I(t)} |\phi_d|^2 + \frac{\gamma_2}{2}\int_{\Gamma_I(T)} |\phi_T|^2 + \frac{\gamma_3}{2}\int_0^T \int_{\Gamma_C} |u|^2;\, \delta\phi \right]\!\!\right] \\ &\quad = -\frac{\gamma_1}{2}\int_0^T \int_{\Gamma_I(t)} \frac{\delta\phi}{|\nabla\phi|}\left(\frac{\partial}{\partial n}\left(|\phi_d|^2\right) + \kappa\,|\phi_d|^2\right) \\ &\qquad - \frac{\gamma_2}{2}\int_{\Gamma_I(T)} \frac{\delta\phi(T)}{|\nabla\phi|}\left(\frac{\partial}{\partial n}\left(|\phi_T|^2\right) + \kappa\,|\phi_T|^2\right). \end{aligned}$$ ◇

(A.1b)

This term does not contribute to the variation of the Lagrangian with ϕ as the domain of integration in this term is fixed. ◇

(A.1c)

The variation of the heat balance in the solid phase is given by (see (B.6))

$$\begin{aligned} \text{(A.1c)} &= -\int_0^T \int_{\partial\Omega_S(t)} \frac{\delta\phi}{|\nabla\phi|}\left(\rho\, c_S\, y_t - k_S\, \triangle y\right) p \\ &= -\int_0^T \int_{\Gamma_I(t)} \frac{\delta\phi}{|\nabla\phi|}\left(\rho\, c_S\, y_t - k_S\, \triangle y\right) p = -\int_0^T \int_{\Gamma_I(t)} \frac{\delta\phi}{|\nabla\phi|} f\, p, \end{aligned}$$

where we have used that $\delta\phi = 0$ on ∂D in the second equality and the last equality holds in the sense of a trace because of (2.1a). ◇

(A.1d)

A similar formula holds for the variation of the heat balance in the fluid phase. The sign changes because the variation is just in the opposite direction compared to the solid phase.

$$\text{(A.1d)} = \int_0^T \int_{\partial\Omega_F(t)} \frac{\delta\phi}{|\nabla\phi|}\left(\rho\, c_F\, y_t - k_F\, \triangle y\right) p$$

4.1.3 Discretizing the Heat Equation with Discontinuous Coefficients

The approximation of the temperature y has to take the moving interface into account, as the coefficients c_S, c_F, k_S and k_F are usually different in the two phases. Rather than employing a moving mesh approach, we use the extended finite element method of Chessa et al. [4]. To account for the phase change across $\Gamma_I(t)$, the standard finite element spaces on a fixed mesh are enriched with additional basis functions. These are continuous but their first derivative has a jump in normal direction to the interface. This spatial discretization is combined with the implicit Euler method in time.

For a detailed description of the forward solver, we refer to [2].

4.2 Discretization of the Adjoint Problem

Equations (3.1a)–(3.1f) with the interface condition (3.1h) have the same structure as (2.1a)–(2.1f) except that the condition that prescribes p on $\Gamma_I(t)$ is now dependent on both time and space. Therefore, it is straightforward to adapt the extended finite element approach from [2] to the spatial discretization of p. Note that the geometry for this adjoint equation is fixed by the solution ϕ of (2.1).

Remark 4.1 *Each step of the implicit Euler scheme for the solution of (2.1) requires the solution of a linear system involving the stiffness matrix $\mathbf{K}^j$, the mass matrix $\mathbf{M}^j$, the pseudo mass matrix $\mathbf{M}^j_{j-1}$ and a matrix $\mathbf{P}^j$ that represents the interface condition (2.1f). The solution of the adjoint equations requires the solution of the same linear systems backwards in time, except that the interface condition (3.1h) is more complicated. Thus, the matrices $\mathbf{K}^j, \mathbf{M}^j$ and $\mathbf{M}^j_{j-1}$ $(j = 1, \ldots, n)$ are stored during the solution of (2.1) and are then invoked for the solution of (3.1), avoiding reassembly.*

One way of discretizing the adjoint Stefan condition (3.1i)–(3.1j) is to go back one step in the derivation of the optimality conditions and to rewrite the adjoint level set equation (A.3) as a PDE on the moving surface $\Gamma_I(t)$. Unfortunately this PDE lacks diffusive terms and thus the available discretization strategies, see [6, 7, 26] to name but a few references, all exhibit stability problems.

As an alternative, we note that all derivatives in the first order conservation law (3.1i) on $\Gamma_I(t)$ are globally defined. Thus, this equation can be directly extended to all of D, or at least to a neighborhood of $\Gamma_I(t)$, by using a constant extension of the terminal condition (3.1j) and the forcing term on the right hand side of (3.1i). We mention that the same idea is used in the context of PDEs on moving surfaces and a finite difference framework in [26].

The resulting conservation law is

$$-\psi_t - \operatorname{div}(\psi\, V) = r \qquad \text{in } D, \tag{4.3a}$$

$$\psi(T) = r_T \qquad \text{in } D, \tag{4.3b}$$

where r and r_T denote constant extensions in normal direction to $\Gamma_I(t)$ of the right hand side of (3.1i) and of the terminal condition (3.1j). To obtain these

constant extensions, we evaluate the forcing terms in (3.1i) and (3.1j) at the interface and feed the resulting data as the boundary data into (4.2), which is then solved by the fast marching method as explained in Section 4.1.2.

We then apply the discontinuous Galerkin scheme of Kuzmin [19] using the space $\mathcal{P}^k_{\text{pw}} := \{w \mid w \in P^k(K) \text{ for all } K \in \mathcal{T}_h\}$ of piecewise polynomials of maximum degree k:

Find $\psi_h(x,t) \in \mathcal{P}^k_{\text{pw}}$ such that

$$0 = -\frac{\partial}{\partial t}\int_K \psi_h\, w_h\, dx - \int_{\partial K} w_h\, \hat{\psi}_h\, V \cdot n\, ds + \int_K \psi_h V \cdot \nabla w_h\, dx \qquad (4.4)$$

for all $w_h \in \mathcal{P}^k_{\text{pw}}$ and for all $K \in \mathcal{T}_h$,

where $\mathcal{T}_h$ is a triangulation of D,

$$\hat{\psi}_h(x,t) = \begin{cases} \psi_h^+(x,t) & V \cdot n < 0,\ x \in \bar{D} \setminus \partial D, \\ \bar{\psi}(x,t) & V \cdot n < 0,\ x \in \partial D, \\ \psi_h^-(x,t) & V \cdot n \geq 0,\ x \in \bar{D}, \end{cases}$$

and $\bar{\psi}$ are Dirichlet boundary data. We apply the same explicit Runge-Kutta scheme as for the forward level set equation to discretize (4.4) in time. The complete algorithm for the adjoint system is given in Algorithm 2.

Remark 4.2 *In Algorithm 2, NB^j denotes the narrow band at time t^j. This quantity is known a-priori from the solution of the forward equation system (2.1). Note that ϕ^j and V^j are given only locally in NB^j and not globally in all of D. This explains the necessity of steps 6 and 11. To map a quantity Ψ from NB^{j-1} to NB^j, we copy the values of Ψ in the vicinity of the interface in NB^{j-1} to the corresponding nodes in NB^j. The fast marching method is then used to extend Ψ to all of NB^j. Simultaneously, the signed distance function to the current interface in NB^j is constructed, see Section 4.1.2.*

Boundary Conditions

The Dirichlet boundary data $\bar{\psi}$ are not given naturally. Rather, artificial boundary conditions have to be specified. To minimize the influence of these conditions, we use a reinitialization procedure in each time step. The adjoint state ψ is evaluated at the interface and then extended to the current narrow band.

Curvature

For the discretization of the curvature κ that arises in the right hand side of (3.1i) and in (3.1j), we make use of the finite element scheme that was proposed by Fried [10]. This approach goes along nicely with our choice of quadratic polynomials for all ansatz and test spaces.

$$\begin{aligned}
&+ \int_0^T \int_{\partial\Omega_S(t)} k_S \tfrac{\partial \delta y}{\partial n}\, p - \int_0^T \int_{\partial\Omega_S(t)} k_S \tfrac{\partial p}{\partial n}\, \delta y + \int_0^T \int_{\Omega_S(t)} k_S \triangle p\, \delta y \\
&- \int_{\Omega_F(T)} \rho\, c_F\, \delta y(T)\, p(T) + \int_0^T \int_{\Omega_F(t)} \rho\, c_F\, p_t\, \delta y - \int_0^T \int_{\Gamma_I(t)} \rho\, c_F\, \delta y\, p\, V \cdot n \\
&+ \int_0^T \int_{\partial\Omega_F(t)} k_F \tfrac{\partial \delta y}{\partial n}\, p - \int_0^T \int_{\partial\Omega_F(t)} k_F \tfrac{\partial p}{\partial n}\, \delta y + \int_0^T \int_{\Omega_F(t)} k_F \triangle p\, \delta y \\
&- \int_0^T \int_{\Gamma_N} k_S \tfrac{\partial \delta y}{\partial n}\, p_N - \int_0^T \int_{\Gamma_C} k_S \tfrac{\partial \delta y}{\partial n}\, p_C \\
&- \int_0^T \int_{\Gamma_I(t)} \delta y\, p_I - \int_0^T \int_{\Gamma_I(t)} \psi \left[k \nabla \delta y\right]_F^S \cdot \nabla \phi.
\end{aligned}$$

Sorting the terms corresponding to their domains of integration and using $n = \frac{\nabla\phi}{|\nabla\phi|}$ on $\Gamma_I(t)$, we get the following condition for the adjoint temperature p:

$$\begin{aligned}
0 = &\int_0^T \int_{\Omega_S(t)} \left(\rho\, c_S\, p_t + k_S \triangle p\right) \delta y + \int_0^T \int_{\Omega_F(t)} \left(\rho\, c_F\, p_t + k_F \triangle p\right) \delta y \\
&- \int_{\Omega_S(T)} \rho\, c_S\, p(T)\, \delta y(T) - \int_{\Omega_F(T)} \rho\, c_F\, p(T)\, \delta y(T) \\
&+ \int_0^T \int_{\Gamma_N} \left(-k_S \tfrac{\partial p}{\partial n}\right) \delta y + k_S \tfrac{\partial \delta y}{\partial n} (p - p_N) \\
&+ \int_0^T \int_{\Gamma_C} \left(-k_S \tfrac{\partial p}{\partial n}\right) \delta y + k_S \tfrac{\partial \delta y}{\partial n} (p - p_C) \\
&+ \int_0^T \int_{\Gamma_I(t)} \left(\rho\, c_S\, p\, V \cdot n - \rho\, c_F\, p\, V \cdot n - k_S \tfrac{\partial p}{\partial n} + k_F \tfrac{\partial p}{\partial n} - p_I\right) \delta y \\
&+ \int_0^T \int_{\Gamma_I(t)} \left(p - \psi\, |\nabla\phi|\right) \left[k \nabla \delta y\right]_F^S \cdot n \qquad \text{for all } \delta y.
\end{aligned}$$

By choosing proper directions of variation δy, equations (3.1a)–(3.1h) follow.

A.2 The Adjoint Stefan Condition

We denote by $D\,[\![H(\phi);\, \delta\phi]\!]$ the variation of $H(\cdot)$ in direction of $\delta\phi$. Using this notation, the derivative of the Lagrangian $\mathcal{L}$ in direction $\delta\phi$ is given by

$$\begin{aligned}
&\mathcal{L}_\phi\, \delta\phi = \\
&\quad D\,[\![J(y,\phi,u);\, \delta\phi]\!] - && \text{(A.1a)} \\
&\quad D\left[\!\!\left[\int_0^T \int_D (-f)\, p;\, \delta\phi\right]\!\!\right] - && \text{(A.1b)} \\
&\quad D\left[\!\!\left[\int_0^T \int_{\Omega_S(t)} \left(\rho\, c_S\, y_t - k_S \triangle y\right) p;\, \delta\phi\right]\!\!\right] - && \text{(A.1c)} \\
&\quad D\left[\!\!\left[\int_0^T \int_{\Omega_F(t)} \left(\rho\, c_F\, y_t - k_F \triangle y\right) p;\, \delta\phi\right]\!\!\right] - && \text{(A.1d)}
\end{aligned}$$

A Formal Derivation of the Optimality Conditions

Throughout this section, we omit the dx, ds and dt for the sake of brevity.

A.1 The Adjoint Temperature

The adjoint temperature equation is the result of taking the derivative $\mathcal{L}_y\,\delta y$ for all directions δy that satisfy $\delta y(x,0)=0$.

As $J_y\,\delta y = 0$, we have

$$\begin{aligned}\mathcal{L}_y\,\delta y = &-\int_0^T\int_{\Omega_S(t)} \left(\rho\, c_S\,\delta y_t - k_S\,\triangle\delta y\right) p - \int_0^T\int_{\Omega_F(t)} \left(\rho\, c_F\,\delta y_t - k_F\,\triangle\delta y\right) p\\ &-\int_0^T\int_{\Gamma_N} k_S\tfrac{\partial\delta y}{\partial n}\,p_N - \int_0^T\int_{\Gamma_C} k_S\tfrac{\partial\delta y}{\partial n}\,p_C\\ &-\int_0^T\int_{\Gamma_I(t)} \delta y\,p_I - \int_0^T\int_{\Gamma_I(t)} \psi\left[k\,\nabla\delta y\right]_F^S\cdot\nabla\phi.\end{aligned}$$

We apply integration by parts in both phases with respect to both time (using (B.3)) and space (using Green's Theorem), to find

$$\begin{aligned}\mathcal{L}_y\,\delta y = &-\int_{\Omega_S(T)}\rho\, c_S\,\delta y(T)\,p(T) + \int_{\Omega_S(0)}\rho\, c_S\,\delta y(0)\,p(0) + \int_0^T\int_{\Omega_S(t)}\rho\, c_S\,p_t\,\delta y\\ &+\int_0^T\int_{\partial\Omega_S(t)}\rho\, c_S\,\delta y\,p\,v_S + \int_0^T\int_{\partial\Omega_S(t)} k_S\tfrac{\partial\delta y}{\partial n}\,p - \int_0^T\int_{\Omega_S(t)} k_S\,\nabla\delta y\nabla p\\ &-\int_{\Omega_F(T)}\rho\, c_F\,\delta y(T)\,p(T) + \int_{\Omega_F(0)}\rho\, c_F\,\delta y(0)\,p(0) + \int_0^T\int_{\Omega_F(t)}\rho\, c_F\,p_t\,\delta y\\ &+\int_0^T\int_{\partial\Omega_F(t)}\rho\, c_F\,\delta y\,p\,v_F + \int_0^T\int_{\partial\Omega_F(t)} k_F\tfrac{\partial\delta y}{\partial n}\,p - \int_0^T\int_{\Omega_F(t)} k_F\,\nabla\delta y\nabla p\\ &-\int_0^T\int_{\Gamma_N} k_S\tfrac{\partial\delta y}{\partial n}\,p_N - \int_0^T\int_{\Gamma_C} k_S\tfrac{\partial\delta y}{\partial n}\,p_C\\ &-\int_0^T\int_{\Gamma_I(t)} \delta y\,p_I - \int_0^T\int_{\Gamma_I(t)} \psi\left[k\,\nabla\delta y\right]_F^S\cdot\nabla\phi,\end{aligned}$$

where v_S and v_F denote the velocity fields corresponding to $\Omega_S(t)$ and $\Omega_F(t)$:

$$\begin{aligned} &v_S = V\cdot n, \quad v_F = -v_s && \text{on } \Gamma_I(t),\\ &v_S = 0 && \text{on } \partial\Omega_S(t)\setminus\Gamma_I(t),\\ &v_F = 0 && \text{on } \partial\Omega_F(t)\setminus\Gamma_I(t).\end{aligned}$$

Using these properties of the normal velocities, $\delta y(x,0)=0$ and applying Green's Theorem once more, we further compute

$$\mathcal{L}_y\,\delta y = -\int_{\Omega_S(T)}\rho\, c_S\,\delta y(T)\,p(T) + \int_0^T\int_{\Omega_S(t)}\rho\, c_S\,p_t\,\delta y + \int_0^T\int_{\Gamma_I(t)}\rho\, c_S\,\delta y\,p\,V\cdot n$$

Efficient Implementation

As for the level set equation (4.1) in the solution of the system (2.1), it suffices to solve (4.4) in a narrow band around the current position of $\Gamma_I(t)$. In accordance with the proposal of Kuzmin [19], we use a Taylor basis for the finite element spaces $\mathcal{P}^k_{\text{pw}}$. In this basis, setting all off-diagonal entries to zero yields a conservative mass lumping strategy. If we use the same basis for solving the level set equation, the mass matrix that is induced by the bilinear form

$$\mathcal{M}(\psi,w) := \int_K \psi\, w\, dx$$

is the same as in the discontinuous Galerkin scheme that we use to solve the level set equation (4.1) in the solution of (2.1). In addition, the system matrix that is induced by the bilinear form

$$\mathcal{K}(\psi,w) := \int_K \psi\, V\cdot\nabla w\, dx$$

is the transpose of the matrix that is induced by the corresponding bilinear form in the level set equation. Thus, as for the adjoint temperature equations, the matrices from solving (4.1) in the forward system are stored and then invoked again during the solution of the adjoint Stefan condition.

Algorithm 2 Solver for the Adjoint Two-Phase Stefan Problem

Input: D, ρ, c_S, c_F, k_S, k_F, L, γ_1, γ_2 and for $j=1,\dots,N_T$:
t^j, $y^j = y(t^j)$, $\phi^j = \phi(t^j)$, $\Gamma_I^j = \Gamma_I(t^j)$, $\text{NB}^j = \text{NB}(t^j)$, $\phi_d^j = \phi_d(t^j)$, ϕ_T
Output: $p^j = p(t^j)$, $\psi^j = \psi(t^j)$, $\quad j=1,\dots,N_T$

1: $j \to N_T$.
2: Initialize p^j and ψ^j in the narrow band NB^j, see (3.1c)–(3.1d) and (3.1j).
3: Evaluate the source term in (3.1i) in NB^j.
4: **while** $j \geq 1$ **do**
5: **if** $\text{NB}^j \neq \text{NB}^{j-1}$ **then**
6: Map ϕ^{j-1} and V^{j-1} from NB^{j-1} to NB^j.
7: **end if**
8: Compute ψ^{j-1} in NB^j.
9: Apply the slope limiter to ψ^{j-1} in NB^j.
10: **if** $\text{NB}^j \neq \text{NB}^{j-1}$ **then**
11: Map ψ^{j-1} from NB^j to NB^{j-1}.
12: **end if**
13: Reinitialize ψ^{j-1} by a constant extension in normal direction in NB^{j-1}.
14: Implement the interface condition (3.1h) by a penalty approach.
15: Solve the adjoint temperature equations to obtain p^{j-1}.
16: Update the source terms in (3.1i).
17: $j \to j-1$.
18: **end while**

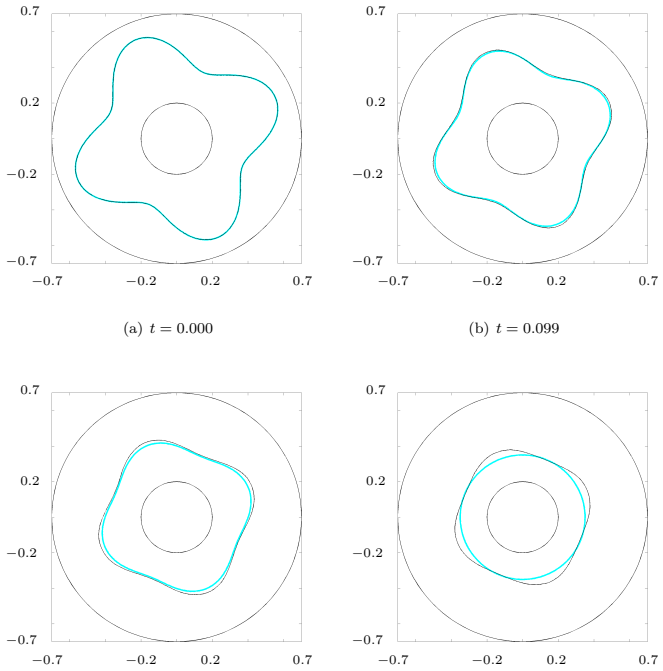

(a) $t = 0.000$ (b) $t = 0.099$

(c) $t = 0.198$ (d) $t = 0.300$

Figure 5.1: The interface position corresponding to the computed control (black, thin line) and the desired motion (cyan, thick line) for the constrained control problem of Section 5.1 at different time steps.

improved by optimization. The predominance of the level set formulation over other approaches is obvious in the solidification problem just mentioned.

The considerable numerical effort that is needed for evolving and for redistancing the level set function, and for constructing the velocity field for the level set update are a shortcoming of the proposed approach. Thus, if the geometric flexibility that our method offers can be dispensed with, a more direct method (as, for instance, the representation of the moving interface as the graph of a function) might be preferable.

The first-order optimality system presented literally translates to the three-dimensional case, except that the curvature κ has to be replaced by the mean curvature. This also holds true for the numerical methods we use. The inclusion of a convection-driven flow in the fluid phase (as, e.g., in [13]) is another potential extension of our approach. Our techniques for the derivation of the optimality conditions are applicable also in this case. The extended finite element approximation can be modified along the lines of [28]. For the optimal control of dendritic solidification, the two-phase Stefan problem must be modified by replacing the isothermal interface condition by the Gibbs-Thomson correction. Consequently, the derivation of the optimality conditions must be adapted to account for the variation of the interface curvature with respect to variations in the level set function. Finally, state constraints, e.g., on the position of the interface, are another challenging extension of the proposed methodology. Their inclusion requires the application of suitable regularization techniques and will be discussed elsewhere.

Acknowledgments

This work was financially supported by FWF (`http://www.fwf.ac.at`) under project grant P19918-N14.

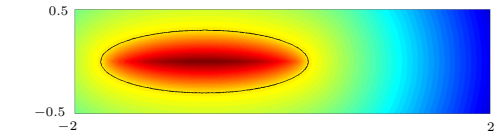

(a) $t = 0.000$

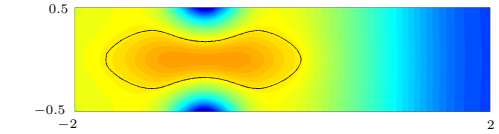

(b) $t = 0.073$

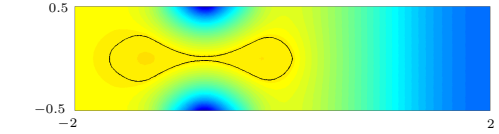

(c) $t = 0.146$

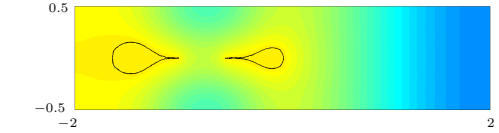

(d) $t = 0.220$

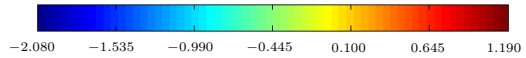

(e) Temperature scale.

Figure 5.9: The temperature distribution and interface evolution corresponding to the computed control for the control problem of Section 5.2 at different time steps.

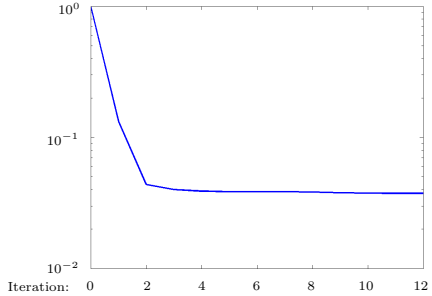

Figure 5.2: The relative cost functional $\widehat{J}(u^j)/\widehat{J}(u^0)$ for the constrained control problem of Section 5.1.

5 Numerical Results

In this section we discuss two examples to highlight the potential of our approach. In the second example, the desired interface motion undergoes a change in topology, which is reproduced by the optimally controled interface. Throughout all computations, we use quadratic finite element spaces on a common triangular mesh for the spatial discretization of the temperature variable y, its adjoint p, the level set function ϕ and its adjoint ψ. In both examples, the constants appearing in (2.1) are chosen as

$$\rho = 1, \quad L = 1, \quad y_M = 0, \quad k_F = \frac{1}{2}, \quad k_S = 1, \quad c_F = c_S = 1.$$

5.1 An Example with Control Constraints

The hold-all we consider in this example is the annulus

$$D = \{(x, y) \in \mathbb{R}^2 \quad | \quad 0.2^2 \leq x^2 + y^2 \leq 0.7^2\}.$$

The control u acts on both parts of the boundary of this domain. The initial configuration is such that the solid phase is adjacent to the outer part of ∂D, i.e., to the circle with radius 0.7 (denoted by $\Gamma_C^{0.7}$), and the fluid phase is adjacent to the inner part of ∂D, i.e., the circle with radius 0.2 (denoted by $\Gamma_C^{0.2}$). The control goal is to track a prescribed interface that shrinks from a flower-like shape at $t = 0$ to a circle at $T = 0.3$, i.e, we consider a solidification problem in which the freezing front should march inwards. The functions ϕ_d and ϕ_T representing the desired interface motion in the cost functional are computed by the fast marching scheme introduced in Section 4.1.2 as the signed distance functions to the zero level sets of the function

$$z(r, \varphi, t) = r - \frac{1 - t}{2} + \frac{0.3 - t}{3} \sin(4\,\varphi),$$

where (r, φ) are the polar coordinates of $x \in D$. We impose the control constraints

$$u \geq 0 \quad \text{on } \Gamma_C^{0,2} \quad \text{and} \quad u \leq 0 \quad \text{on } \Gamma_C^{0,7}.$$

The domain is discretized using 3384 triangles and we make 200 time steps. Moreover, we use the parameters $\gamma_1 = \gamma_2 = 1$, $\gamma_3 = 0.01$ in the cost functional and apply Algorithm 1 with the initial guess $u^0 = 0$. The results after 12 gradient steps are reported in Figures 5.1–5.5.

Figure 5.1 shows the positions of the controled and the desired interfaces at different instances of time. The controled interface is much closer to the desired interface position than in the uncontroled case (not shown). Figure 5.2 shows the evolution of the relative cost functional $\widehat{J}(u^j)/\widehat{J}(u^0)$ in a semi-logarithmic scale. We observe the characteristic behavior of gradient based optimization methods: The convergence is fast in the beginning of the iteration, but after a few steps the procedure slows down. The computed optimal control and the corresponding temperature distribution are shown in Figure 5.3 and Figure 5.5 at the same instances of time as the interface positions in Figure 5.1. We observe that, except for $t = T = 0.3$, the control constraint on $\Gamma_C^{0,7}$ is never active. The constraint on $\Gamma_C^{0,2}$ is only active towards the end of the process, see Figure 5.4. Due to the relations (3.1c), (3.1d) and (3.2), the control u must vanish at $t = T$. This is indeed the case, as can be seen in Figure 5.3(d).

5.2 An Example with a Change of Topology

One of the distinguishing features of the level set method is its capability to handle changes of topology. The example we discuss in this section demonstrates that our optimal control approach inherits this property. We consider the rectangular hold-all $D = [-2, 2] \times [-0.5, 0.5]$. The initial configuration is such that the solid phase, which is adjacent to ∂D, completely encloses the fluid phase. As in Section 5.1, the desired interface motion corresponds to an inwards solidification, starting from an ellipse-like shape at $t = 0$. A pinch-off should occur at $t \approx 0.134$. The level set functions ϕ_d and ϕ_T which encode the desired interface evolution are taken as the signed distance functions to the evolving interface obtained during a simulation run with given Neumann temperature boundary data. Fast marching reinitialization as described in Section 4.1.2 is used.

The boundary is decomposed into two parts $\Gamma(t) = \Gamma_N \cup \Gamma_C$ that are defined by

$$\Gamma_N = [-0.5, 0.5] \times \{-2\} \cup [-0.5, 0.5] \times \{2\},$$
$$\Gamma_C = [-2, 2] \times \{-0.5\} \cup [2, 2] \times \{0.5\}.$$

As in Section 5.1, we impose the control constraint

$$u \leq 0 \qquad \text{on } \Gamma_C.$$

The Neumann data on Γ_N are homogeneous. The domain is discretized using 4096 triangles and we make 220 time steps in the interval $[0, 0.22]$. We use the

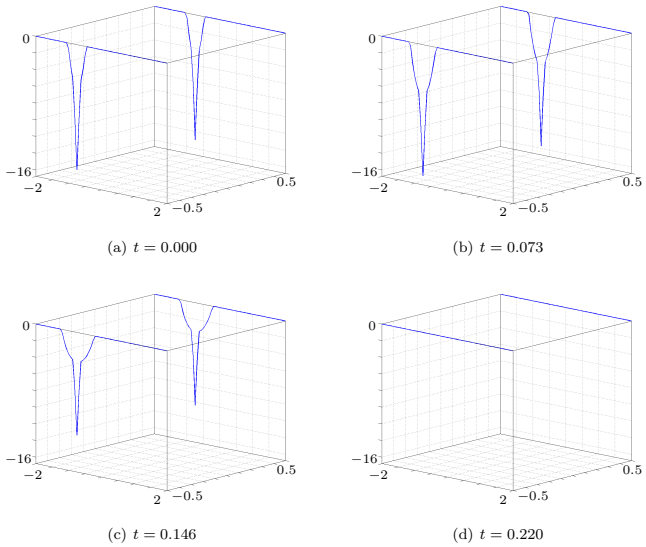

(a) $t = 0.000$ (b) $t = 0.073$

(c) $t = 0.146$ (d) $t = 0.220$

Figure 5.8: The computed control for the control problem of Section 5.2 at different time steps.

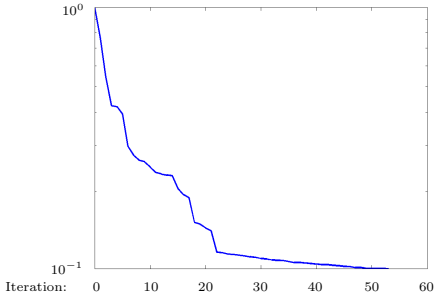

Figure 5.7: The relative cost functional $\widehat{J}(u^j)/\widehat{J}(u^0)$ for the control problem of Section 5.2.

parameters $\gamma_1 = 8$, $\gamma_2 = 1$, $\gamma_3 = 10^{-4}$ in the cost functional and apply Algorithm 1 with an initial guess u^0 which is given by a scaled down version of the Neumann data used to generate the desired interface motion. The results after 53 gradient steps are reported in Figures 5.6–5.9. Figure 5.6 shows that the controled interface follows the desired interface positions very closely. In particular, it demonstrates that our optimal control approach can handle changes of topology. As in Section 5.1, the behavior of the relative cost functional (shown in a semi-logarithmic scale in Figure 5.7) is again typcial for gradient methods: After a good progress in the beginning the optimization slows down.

6 Discussion and Conclusion

The level set representation of the fluid-solid interface provides enough geometric flexibility for handling closed curves and for capturing changes of topology in the simulation of the forward problem. Our optimal control approach inherits this beneficial property as demonstrated by the numerical examples. The proposed methodology extends to cases in which the interface touches the boundary of the given hold-all as it is the case in, e.g., VGF crystal growth. However, this case requires some changes in the optimality conditions. The corresponding results will be published elsewhere.

A mathematical motivation for utilizing the level set method is that during the iterative numerical solution of the optimal control problem topological changes may appear in the interface. Casting problems and crystal growth processes represent potential applications of the proposed optimal control approach. Chessa et al. [4] consider the solidification of a two-dimensional casting model where the interface evolution features closed parts and topological changes. The optimization of such casting processes to ensure that the freezing front follows a desired trajectory is desirable for various reasons. Among other goals, the quality of the final product and the length of the production cycle might be significantly

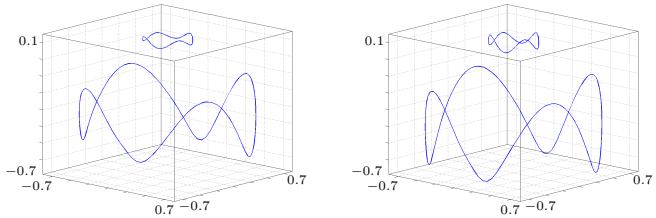

(a) $t = 0.000$ (b) $t = 0.099$

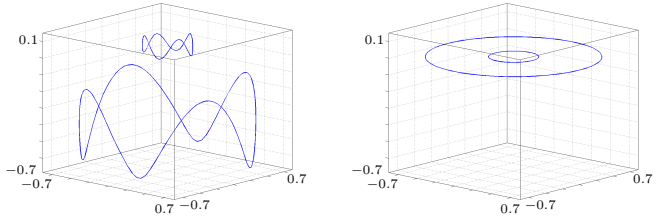

(c) $t = 0.198$ (d) $t = 0.300$

Figure 5.3: The computed control for the constrained control problem of Section 5.1 at different time steps.

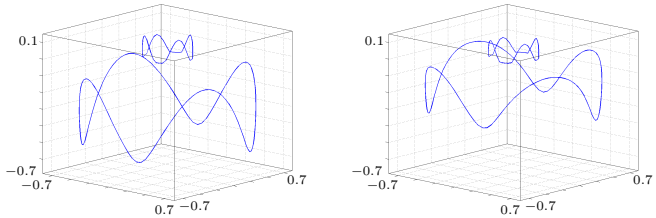

(a) $t = 0.255$ (b) $t = 0.285$

Figure 5.4: Activity of the control constraint the control problem of Section 5.1 at time steps $t \in \{0.255, 0.285\}$.

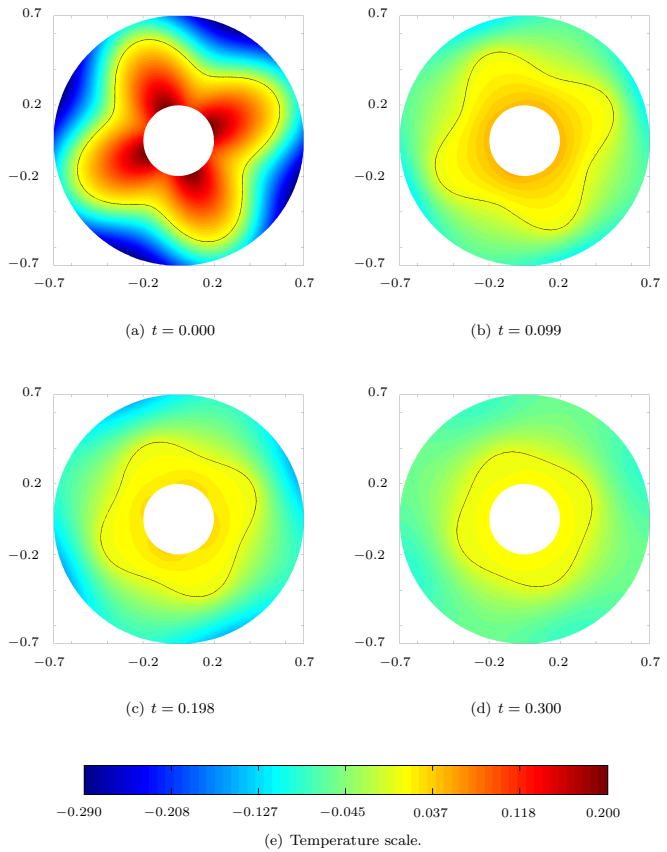

(a) $t = 0.000$ (b) $t = 0.099$

(c) $t = 0.198$ (d) $t = 0.300$

(e) Temperature scale.

Figure 5.5: The temperature distribution and interface evolution corresponding to the computed control for the constrained control problem of Section 5.1 at different time steps.

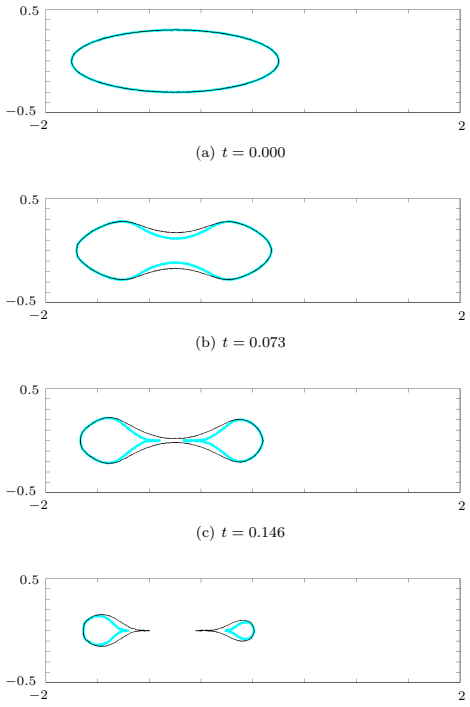

(a) $t = 0.000$

(b) $t = 0.073$

(c) $t = 0.146$

(d) $t = 0.220$

Figure 5.6: The interface position corresponding to the computed control (black, thin line) and the desired motion (cyan, thick line) for the control problem of Section 5.2 at different time steps.